

# Transient Pulse Formation in Jasmonate Signaling Pathway

Subhasis Banerjee and Indrani Bose

June 8, 2018

Department of Physics, Bose Institute, 93/1, A. P. C. Road, Kolkata 700009.

## Abstract

The jasmonate (JA) signaling pathway in plants is activated as defense response to a number of stresses like attacks by pests or pathogens and wounding by animals. Some recent experiments provide significant new knowledge on the molecular detail and connectivity of the pathway. The pathway has two major components in the form of feedback loops, one negative and the other positive. We construct a minimal mathematical model, incorporating the feedback loops, to study the dynamics of the JA signaling pathway. The model exhibits transient gene expression activity in the form of JA pulses in agreement with experimental observations. The dependence of the pulse amplitude, duration and peak time on the key parameters of the model is determined computationally. The deterministic and stochastic aspects of the pathway dynamics are investigated using both the full mathematical model as well as a reduced version of it. We also compare the mechanism of pulse formation with the known mechanisms of pulse generation in some bacterial and viral systems.

## 1 Introduction

Plants are frequently subjected to a number of stresses like attacks by pests or pathogens and wounding by animals which cause damage to the plant cells. In higher plants, the response to damages is mediated via the jasmonate (JA) signaling pathway [1, 2, 3, 4]. On activation of the pathway, there is a rapid but transient accumulation of JAs in the infected/wounded cells. This leads to the expression of JA- responsive genes involved in defense-related processes. More generally, JAs are produced in response to a number of biotic and abiotic stresses and also play active roles in regulating developmental processes. The JA signaling pathway is an integral component of a plant's defense system but till recently there were large gaps in our understanding of how the pathway operates. Two experimental studies [5, 6], carried out on the model plant *A. thaliana*, now provide significant knowledge on the molecular details of the signaling pathway which helps in the elucidation of its functional features.

Figure 1 shows a schematic diagram of the core components of the JA signaling pathway [7]. JA responses typically involve changes in the expressions of hundreds of genes [1]. Transcription factors (TFs) like MYC2 regulate the expressions of JA-responsive genes including those promoting JA biosynthesis. Under normal circumstances, MYC2 is non-functional due to binding by the JASMONATE-ZIM-domain (JAZ) repressor proteins and the JA levels in cells are low. On

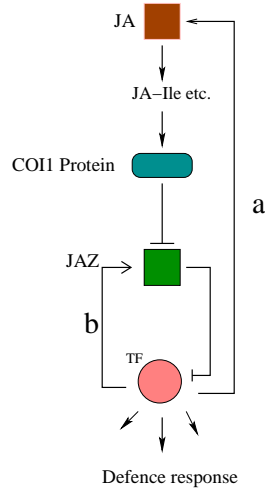


Figure 1: Core components of the JA signaling pathway [7]. Transcription factor (TF), MYC2, activates the synthesis of both JA and JAZ. The arrow sign denotes activation and the hammerhead sign repression. The function of the components is described in the text.

wounding, damage-induced signals initiate JA biosynthesis so that JA levels are elevated in cells. This results in the formation of the jasmonate-L-isoleucine (JA-Ile) complex which mediates the binding of CORONATINE INSENSITIVE 1(COI1) and JAZ proteins. COI1 forms part of an enzyme complex  $SCF^{COI1}$  which tags the bound JAZ proteins with ubiquitin marking them for destruction. The degradation of JAZ proteins liberates the TF MYC2 and possibly other TFs involved in JA-induced gene expression. Thus, enhanced JA levels result in the activation of the JA signaling pathway through the destruction of the JAZ proteins, the repressors of the pathway. There are two primary regulatory loops **a** and **b** in the JA signaling pathway (figure 1). Loop **b** is the newly discovered [5, 6, 7] negative feedback loop involving MYC2 and JAZ proteins. MYC2 activates the synthesis of the JAZ proteins whereas JAZ binds MYC2 and inhibits its activity as a TF. The synthesis of JA is autoactivating via the positive feedback loop **a** since a JA signal gives rise to free MYC2 which in turn activates the genes responsible for JA biosynthesis. The combination of positive and negative feedback loops **a** and **b** gives rise to transient gene expression activity so that JA accumulation is in the form of a pulse.

In this paper, we develop a minimal mathematical model incorporating the core components of the JA signaling pathway [7] shown in figure 1. We specially investigate how the regulatory loops affect the gene expression dynamics. Based on our results, we make testable predictions on the dependence of the amplitude and duration of the transient JA pulses on the key parameters of the model. There are other examples of transient pulse formation in gene regulatory networks which include the development of competence in the bacterial population *B. subtilis* [8, 9, 10], infection of a host cell by the HIV-1 virus with a subsequent choice between two distinct cell fates, latency and lysis [11, 12, 13], and regulation of the *Salmonella* pathogenicity by the PhoP/PhoQ two-component system [14]. The transient pulse in each case is that of a key regulatory protein : ComK (competence development ), Tat (HIV-1 virus ) and phosphorylated PhoP ( *salmonella* pathogenicity ). The regulatory proteins reach sufficiently high concentrations in the peak regions of the pulses to activate competence development in *B. subtilis*, lysis in the host cell infected by the HIV-1 virus and virulence in the case of *salmonella* pathogens. In a *B.subtilis* population subjected to stress, competence develops in a fraction of cells involving the uptake of DNA from the environment and its integration into the bacterial genome. This confers new traits on the

bacteria which helps in bacterial survival under stress. A combination of mathematical modeling and experimental approaches provide new insight on the mechanisms of pulse formation in the cases considered. The mechanisms differ in detail but there is one common feature, namely, the presence of a positive feedback loop involving the key regulatory protein.

The transient nature of a regulatory pulse is determined by two opposing influences. In the case of *B.subtilis*, the competence events are generated by two feedback loops, one positive and the other negative. Positive feedback amplifies the ComK level whereas negative feedback brings it down to that of the vegetative (non-competent) state. The HIV circuit has been proposed to function like a feedback resistor [12] to explain transient Tat activity. Forward reactions ( e.g., acetylation of Tat ) constituting the positive feedback loop amplify the Tat level whereas stronger back reactions (deacetylation, degradation and unbinding of the regulatory molecules) eventually deactivate the circuit. The two-component PhoP/PhoQ system controlling salmonella pathogenicity operates on similar principles [14]. These known mechanisms of transient pulse formation provide the motivation for identifying the mechanism underlying transient pulse generation in the JA signaling pathway. In section 2, we develop a minimal mathematical model of the JA signaling pathway to study how JA pulses are formed. The dependence of the pulse characteristics like amplitude, duration and peak time on the key parameters of the model is computed. We further consider a reduced version of the general model to capture the essential features of the dynamics of pulse formation. In section 3, we investigate the dynamics of the JA signaling pathway using stochastic approaches. Section 4 contains concluding remarks and a comparison of the mechanisms of pulse formation in different signaling pathways.

## 2 Mathematical model of JA-Signaling Pathway

In the deterministic approach, the dynamics of the JA-signaling pathway are determined by a set of differential equations describing the rates of change in the concentrations of the key molecular components in the pathway (figure1) with respect to time. The biochemical reactions to be considered are:



$JZ$ ,  $JA$  and  $M$  denote the molecular species JAZ, JA and MYC2.  $IL$ ,  $M\_JZ$ ,  $JAIL$  and  $JZ\_JAIL$  represent isoleucine, the bound complex of JAZ and MYC2, the JA-Ile complex and the complex of JAZ with JA-Ile respectively. The same symbols represent the concentrations of the respective molecular species. The rate constants  $k_1$ - $k_7$  are associated with the different forward and backward reactions. Two other reactions which we take into account describe the degradation of JAZ and JA. As mentioned in the Introduction, we develop a minimal model of the JA-signaling pathway to probe the mechanism of JA pulse formation. In the following, we point out the simplifications made in developing the model and the justifications thereof. JA and JA-Ile levels are known to increase dramatically (  $\sim 25$  fold increase within five minutes of tissue injury ) in response to both mechanical wounding and herbivory [15]. The remarkable speed of response suggests that

all the biosynthetic enzymes required for the production of JA/JA-Ile are available in the resting cells. In our minimal model, the enzymatic activity is implicit in the effective reactions considered with the enzyme concentrations absorbed in the appropriate rate constants. The conjugation of JA to Ile is mediated by the enzyme JASMONATE RESISTANT1 (JAR1) [16] which is described by the effective binding reaction in equation (2). Recent reports [1, 5, 6, 7, 17] have conclusively established that JA-Ile directly induces the binding of the JAZ proteins with COI1 which results in the destruction of the repressor proteins. These processes are combined in the effective reactions contained in equation (3). Experimental evidence of the direct binding between COI1 and JA-Ile has not been reported so far [17] though a molecular mechanism for the formation of the bound complex of JA-Ile, COI1 and JAZ has been proposed recently [18, 19]. The JAZ proteins are distinguished by the presence of a highly conserved Jas domain which mediates protein-protein interactions with both TFs like MYC2 and COI1 [18]. It appears that the COI1 and MYC2 proteins compete for interaction with the Jas motif [17]. The presence of JA determines the outcome of the competition since the COI1-Jas domain interaction requires the presence of JA-Ile whereas MYC2 interacts in a hormone-independent manner.

Apart from the reactions (1)-(3), the model also takes into account the synthesis of JAZ proteins through the TF (MYC2) regulated expression of the JAZ genes and the biosynthesis of JA. We do not model the full octadecanoid pathway for JA biosynthesis which is activated by damage-induced signals [1, 20]. One major feature of the pathway is that the JA biosynthesis genes are regulated by TFs like MYC2, thus constituting a positive feedback loop. In recent studies [21] MYC2 has been identified as a transcriptional activator of the JA biosynthesis gene *LOX3*. This finding matches earlier observations [22] that JA-induced *LOX3* expression is reduced in the MYC2-defective mutant *jin1*. The differential rate equations of the model are given by:

$$\frac{d(JZ)}{dt} = \frac{\beta_1 M}{Km_1 + M} + k_2 M_{-}JZ - k_1 JZ \cdot M + k_6 JZ_{-}JAIL - k_5 JZ \cdot JAIL - \gamma_1 JZ \quad (4)$$

$$\frac{d(JA)}{dt} = \frac{\beta_2 M}{Km_2 + M} + k_4 JAIL - k_3 JA \cdot IL - \gamma_2 JA \quad (5)$$

$$\frac{d(M_{-}JZ)}{dt} = k_1 M \cdot JZ - k_2 M_{-}JZ \quad (6)$$

$$\frac{d(JAIL)}{dt} = k_3 JA \cdot IL - k_4 JAIL + (k_6 + k_7) JZ_{-}JAIL - k_5 JAIL \cdot JZ \quad (7)$$

$$\frac{d(JZ_{-}JAIL)}{dt} = k_5 JZ \cdot JAIL - (k_6 + k_7) JZ_{-}JAIL \quad (8)$$

The first term in equation (4) describes JAZ synthesis due to MYC2-regulated gene expression. The TF binding/unbinding events occur on a time scale much faster than that of protein synthesis and degradation. One can thus assume that steady state conditions prevail in the formation of the TF-gene complex. The MYC2-mediated synthesis of JA is represented as an effective process by the first term in equation (5). The rate constants  $\beta_1$  and  $\beta_2$  denote the maximum rates of JAZ and JA synthesis. The synthesis rate is half-maximal when  $Km_1, Km_2 = M$ , the concentration of the regulating protein MYC2. There are two conservation equations.

$$M_t = M + M_{-}JZ \quad (9)$$

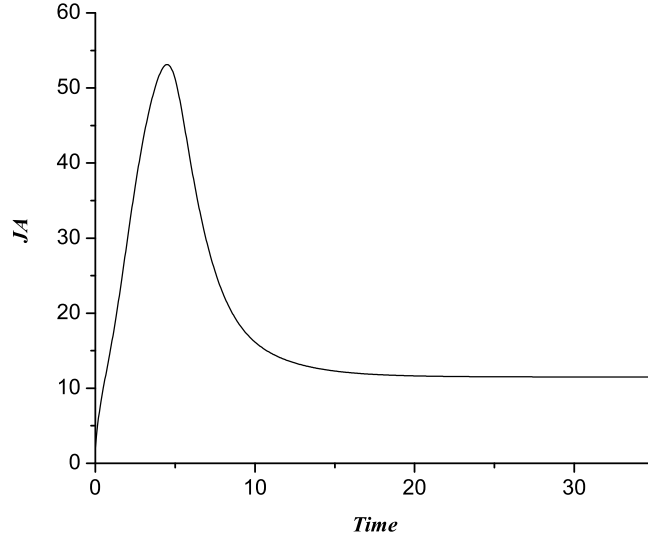


Figure 2: Transient pulse of JA versus time in hours.  $JA$  has the unit of concentration.

$$IL_t = Il + JAIL + JZ\_JAIL \quad (10)$$

where  $M_t$  and  $IL_t$  are the total concentrations of MYC2 and isoleucine respectively in free as well as bound forms. The rate constants  $\gamma_1$  and  $\gamma_2$  in equations (4)-(5) are the degradation rate constants for JAZ and JA.

We now investigate whether the mathematical model, described in terms of equations (1)-(10), can reproduce transient pulse formation consistent with experimental observations in wounded plants [15, 23, 24]. Indeed, we find that over a wide range of parameter values JA accumulation is in the form of a pulse. Figure 2 shows one such transient pulse for the parameter values  $\beta_1 = 30$ ,  $\beta_2 = 30$ ,  $k_1 = 0.2$ ,  $k_2 = 0.001$ ,  $k_3 = 0.1$ ,  $k_4 = 0.1$ ,  $k_5 = 0.1$ ,  $k_6 = 1.0$ ,  $k_7 = 1.0$ ,  $Km_1 = 1$ ,  $Km_2 = 1$ ,  $\gamma_1 = 0.1$ ,  $\gamma_2 = 0.4$  in appropriate units. The concentration of JA initially rises with time, reaches a maximum value and then decays to reach a low steady state value. The transient nature of the pulse is an outcome of competing negative and positive feedback loops. An individual pulse is distinguished by quantities like amplitude (maximal value), temporal duration and peak time,  $t_m$  i.e., the time at which the maximal value of the variable being measured is achieved. The duration time  $t_D$  is measured as  $t_D = t_{max2} - t_{max1}$ , where  $t_{max1}$  and  $t_{max2}$  are respectively the time points at which the rates of increase and decrease attain their largest values. Since positive feedback has the effect of amplifying JA levels/activity, the amplitude of a pulse can be increased by strengthening the positive feedback. Figure 3 shows how the JA concentration changes as a function of time for different values of  $\beta_2$ , the maximal rate of JA synthesis. The rest of the parameters have the same values as in the case of figure 2. Figure 2 is obtained by solving the differential equations (4) - (8) with the initial ( $t = 0$ ) conditions  $JA = 2$ ,  $M = 100$  and  $Il = 20$ . The values assumed for  $M_t$  and  $IL_t$  are  $M_t = 200$  and  $IL_t = 20$ . An initial dose of JA molecules is essential to free MYC2 so that activation of the JA signaling pathway is possible. Wounding signals stimulate the biosynthesis of JA which provides the initial JA input. Once free MYC2 is available, JA biosynthesis is further stimulated via the positive feedback loop shown in figure 1. Our model calculations start with the state which already has free MYC2 and we focus on how the activation and deactivation of the

Table 1: Parameters, their meanings and defining formulae (the units are given in brackets,  $[c]$ =concentration,  $[t]$ =time)

Parameter	Meaning/defining formula
$k_1, k_2$ $(\frac{1}{[c][t]}, \frac{1}{[t]})$	Rate constants for the formation and dissociation respectively of the bound complex ( $M\_JZ$ ) of JAZ and MYC2 proteins (defined in equation (1))
$k_3, k_4$ $(\frac{1}{[c][t]}, \frac{1}{[t]})$	Rate constants for the formation and dissociation of the bound complex ( $JAIL$ ) of JA with IL (defined in equation (20))
$k_5, k_6$ $(\frac{1}{[c][t]}, \frac{1}{[t]})$	Rate constants for the formation and dissociation respectively of the complex $JZ\_JAIL$ of JAZ proteins with $JAIL$ . (defined in equation (3))
$k_7$ $(\frac{1}{[t]})$	Rate constant for ubiquitin-mediated degradation of JAZ proteins (defined in equation (3))
$\gamma_1, \gamma_2$ $(\frac{1}{[t]}, \frac{1}{[t]})$	Degradation rate constants of JAZ proteins and JA respectively (defined in equations (4) and (5))
$\beta_1, \beta_2$ $(\frac{[c]}{[t]}, \frac{[c]}{[t]})$	Maximum rates of JAZ and JA synthesis (defined in equations (4) and (5))
$Km_1, Km_2$ $([c], [c])$	Synthesis rate of JAZ and JA is half-maximal when $Km_1, Km_2 = M$ , the concentrations of the regulatory protein $MYC2$
$M_t, IL_t$ $([c], [c])$	Total concentrations of MYC2 and isoeucine respectively which are defined in equations (9) and (10)

JA pulse occurs due to the dynamics of the coupled positive and negative feedback loops. If the initial JA and MYC2 values are increased, the amplitude of the transient JA pulse increases. As  $\beta_2$  becomes larger, there is a greater accumulation of JA resulting in an increase in the amplitude of the JA pulse.

Figure 4 shows the variation of JA concentration versus time for different values of  $\beta_1$ , the maximal rate of JAZ synthesis. The other parameter values are the same as in the case of figure 2. With increasing values of  $\beta_1$ , the amount of JAZ proteins goes up and there is more repression of MYC2 activity. This leads to a reduction in the duration of the JA pulse. The change in the amplitude is, however, not as prominent as that when  $\beta_2$  is varied. This is more evident in figures 5(a) and (b) in which the amplitude of the JA pulse is plotted against  $\beta_1$  and  $\beta_2$ , respectively keeping the other parameter values the same as in the case of figure 2. Figures 5(c) and (d) exhibit the variation of the peak time  $t_m$  versus  $\beta_1$  and  $\beta_2$  respectively. The magnitude of  $t_m$  decreases considerably as  $\beta_1$  is increased. The dependence of  $t_m$  on  $\beta_2$  is, however, insignificant. Figures 5 (e) and (f) show a plot of  $t_D$ , the duration of the JA pulse, versus  $\beta_1$  and  $\beta_2$ . The dependence of  $t_D$  on  $\beta_2$  is negligible. Figure 6 shows the variation of JA concentration versus time as the

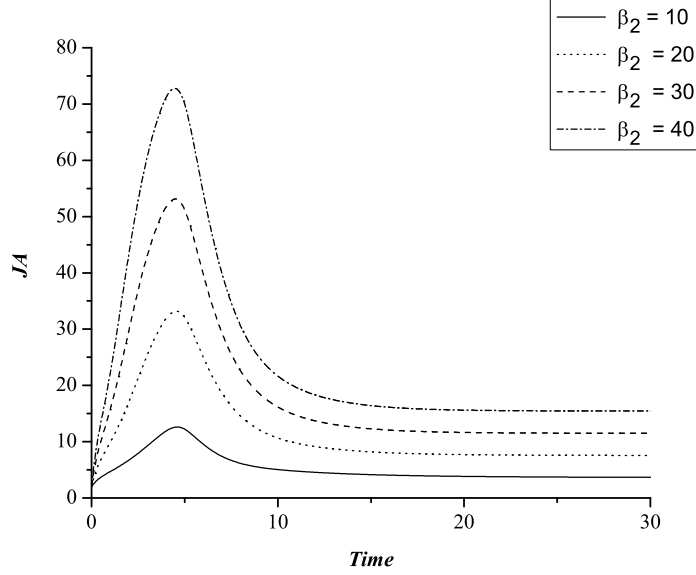


Figure 3: Variation of JA versus time in hours for values of  $\beta_2 = 10, 20, 30$  and  $40$ . The peak height of the pulse increases for increasing values of  $\beta_2$ .  $JA$  has the unit of concentration.

degradation rate constant  $\gamma_2$  is changed. Similar figures may be obtained by varying the other parameters of the model. For the set of parameter values considered, the most prominent changes are obtained by varying the maximum synthesis rates  $\beta_1$  and  $\beta_2$ . Figures 3-6 have been obtained with the total concentrations fixed at the values  $M_t = 200$ , and  $IL_t = 20$  in appropriate units. Table 1 lists all the parameters of the dynamical model, their description as well as units. The different parameter units are expressed in terms of concentration ([c]) and time ([t]) units. There are presently no methods available to record the cellular concentrations of JA, JA-Ile etc., the quantities measured are amounts per gram fresh weight. In our model study, the JA amounts have the units of concentration.

To analyse the features of the model better, we reduce it to a two-variable model described by rate equations which are in dimensionless form. The reduction rests on the fact that the molecular complexes  $M_{-}JZ$ ,  $JA_{IL}$  and  $JZ_{-}JA_{IL}$  attain their steady state concentrations on timescales which are comparably shorter than those over which the JA and JAZ reach their steady state concentrations. Therefore, one can take the time derivatives in equations (6)-(8) to be zero so that the complexes  $M_{-}JZ$ ,  $JA_{IL}$  and  $JZ_{-}JA_{IL}$ , attain their steady state concentrations. The reduced model is described by the rate equations

$$\frac{d(JZ)}{dt} = \frac{\beta_1 M}{Km_1 + M} - \delta_{JZ} \frac{JA \cdot JZ}{JA + K1 + \frac{JZ}{\Gamma} \cdot JA} - \gamma_1 JZ \quad (11)$$

$$\frac{d(JA)}{dt} = \frac{\beta_2 M}{Km_2 + M} - \gamma_2 JA \quad (12)$$

with  $\Gamma = \frac{k_6+k_7}{k_5}$ ,  $K1 = \frac{k_4}{k_3}$  and  $\delta_{JZ} = \frac{k_7 IL_t}{\Gamma}$ . Also,  $M_t = M(1 + \frac{k_1}{k_2} JZ)$  and  $IL_t = IL(1 + \frac{k_3}{k_4} JA(1 + \frac{JZ}{\Gamma}))$ . Rescaling time with  $\delta_{JZ}$  and the concentrations JZ and JA with  $\Gamma$ , we obtain the dimensionless rate equations:

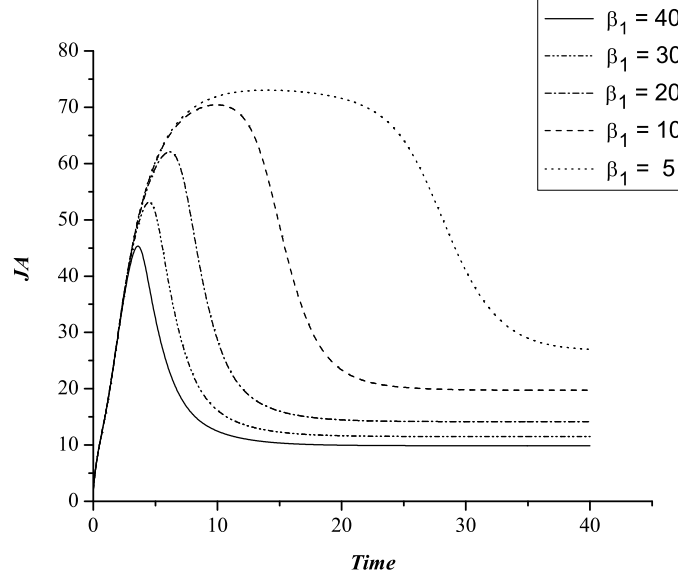


Figure 4: Variation of  $JA$  versus time for different values of  $\beta_1 = 5, 10, 20, 30$  and  $40$ .

$$\frac{d(JZ)}{dt} = \frac{b_1}{kn_1(1 + K' JZ) + 1} - \frac{JA \cdot JZ}{JA + K2 + JA \cdot JZ} - \delta_1 JZ \quad (13)$$

$$\frac{d(JA)}{dt} = \frac{b_2}{kn_2(1 + K' JZ)} - \delta_2 JA \quad (14)$$

where  $t$ ,  $JZ$  and  $JA$  are now dimensionless variables with the dimensionless parameters shown in Table 2.

Equations (13)-(14) can be further simplified to

$$\frac{d(JZ)}{dt} = \frac{\alpha_1}{1 + \mu_1 JZ} - \frac{JA \cdot JZ}{JA + K2 + JA \cdot JZ} - \delta_1 JZ \quad (15)$$

$$\frac{d(JA)}{dt} = \frac{\alpha_2}{1 + \mu_2 JZ} - \delta_2 JA \quad (16)$$

The parameters  $\alpha_1, \alpha_2, \mu_1$  and  $\mu_2$  are defined in Table 2. We first consider the case  $\delta_1 = 0$  as degradation of the JAZ proteins mostly occurs via the second term in Eq.(13) describing ubiquitin-mediated degradation on the binding of the SCF<sup>COI1</sup> complex to JAZ proteins. The steady state of the dynamical system is obtained by putting the temporal rates of change,  $\frac{d(JZ)}{dt}$  and  $\frac{d(JA)}{dt}$ , to be zero. There is only one physical steady state solution given by

$$(JZ)_s = \frac{A + \sqrt{A^2 + 4\alpha_1\alpha_3\mu_1(\alpha_3 + K2)}}{2\alpha_3\mu_1} \quad A = \alpha_1\alpha_3 + \alpha_1K2\mu_2 - \alpha_3 \quad (17)$$

$$(JA)_s = \frac{\alpha_2}{1 + \mu_2(JZ)_s} \quad \alpha_3 = \frac{\alpha_2}{\delta_2} \quad (18)$$



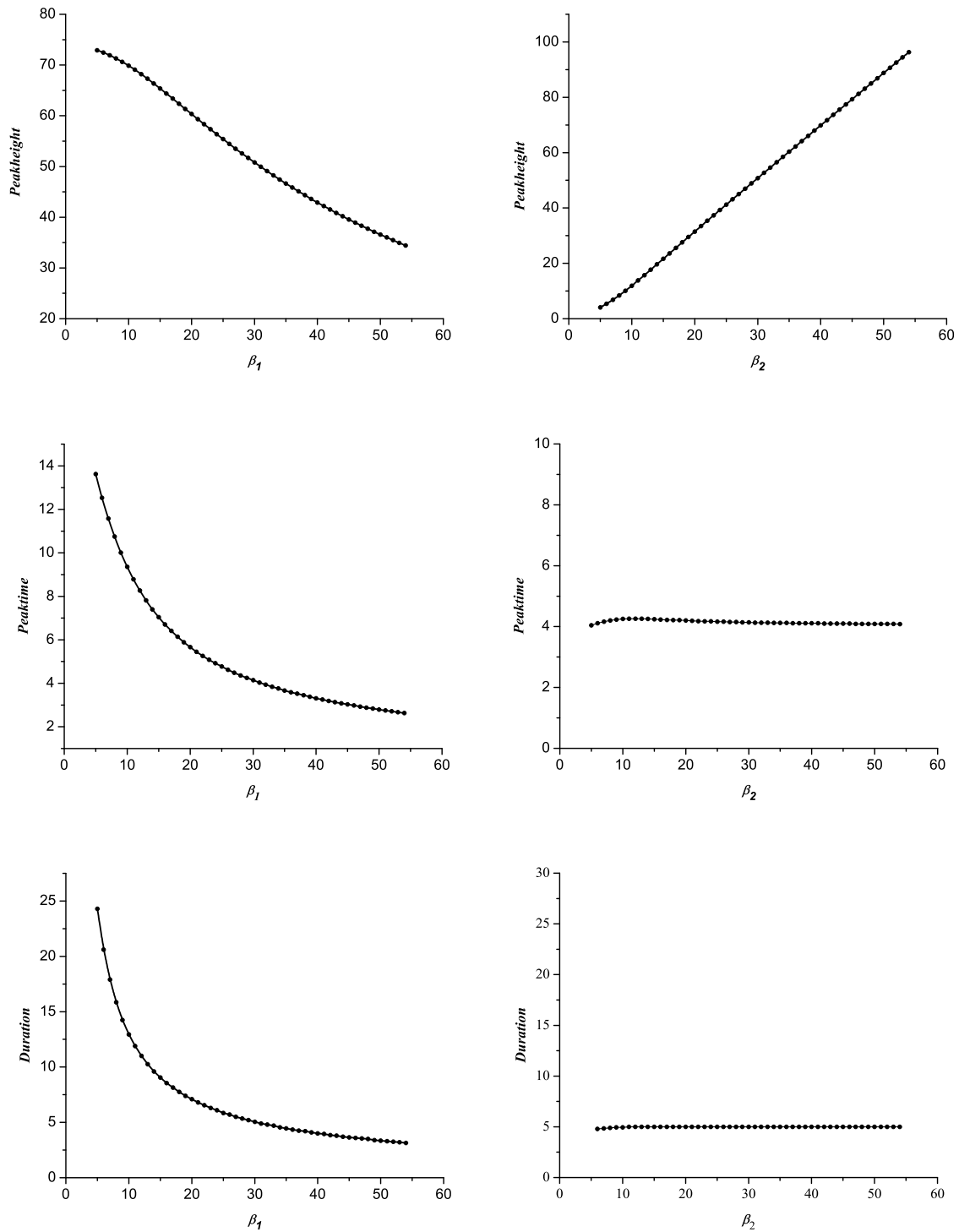


Figure 5: Amplitude of JA pulse versus (a)  $\beta_1$  and (b)  $\beta_2$  ; Peak time  $t_m$  in hours of the JA pulse versus (c)  $\beta_1$  and (d)  $\beta_2$ ; Duration  $t_D$  in hours of JA pulse versus (e)  $\beta_1$  and  $\beta_2$ .

Table 2: Rescaled parameters and their definitions

Parameter	Definition	Abbreviation
$b_1$	$\frac{\beta_1}{\delta_{JZ} \Gamma}$	$\delta_{JZ} = \frac{k_7 IL_t}{\Gamma}$
$b_2$	$\frac{\beta_2}{\delta_{JZ} \Gamma}$	$\Gamma = \frac{k_6+k_7}{k_5}$
$kn_1$	$\frac{Km_1}{M_t}$	$M_t = M(1 + \frac{k_1}{k_2} JZ)$
$kn_2$	$\frac{Km_2}{M_t}$	$IL_t = IL(1 + \frac{k_3}{k_4} JA(1 + \frac{JZ}{\Gamma}))$
$K'$	$\Gamma \frac{k_1}{k_2}$	
$K2$	$\frac{K1}{\Gamma}$	
$\delta_1$	$\frac{\gamma_1}{\delta_{JZ}}$	
$\delta_2$	$\frac{\gamma_2}{\delta_{JZ}}$	
$\alpha_1$	$\frac{b_1}{kn_1+1}$	
$\alpha_2$	$\frac{b_2}{kn_2+1}$	
$\mu_1$	$\frac{kn_1 K'}{(kn_1+1)}$	
$\mu_2$	$\frac{kn_2 K'}{(kn_2+1)}$	

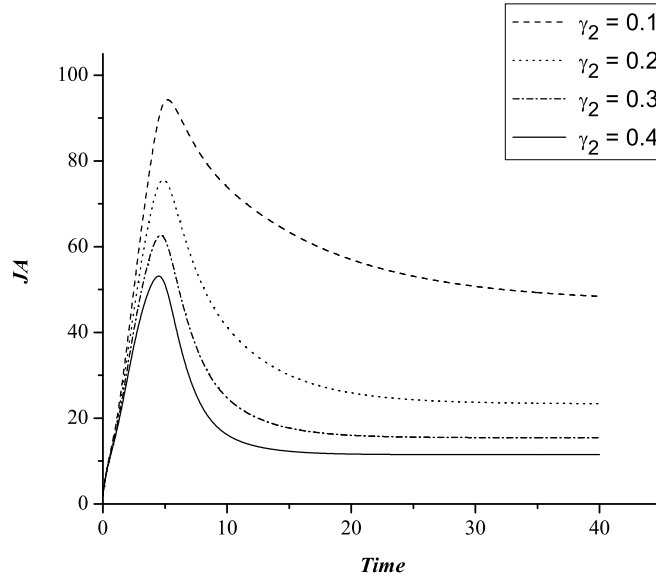


Figure 6: Variation of  $JA$  versus time in hours for different values  $\gamma_2 = 0.1, 0.2, 0.3$  and  $0.4$  of the degradation rate constant. The amplitude of the  $JA$  pulse decreases for increasing value of  $\gamma_2$ .  $JA$  has the unit of concentration.

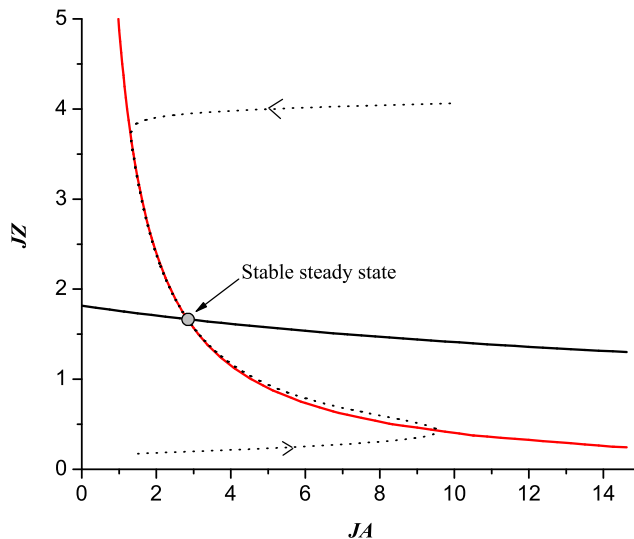


Figure 7: Phase portrait defined by equations (15) and (16). The solid lines represent the nullclines( $\frac{d(JA)}{dt} = 0$ (red),  $\frac{d(JZ)}{dt} = 0$ (black)) intersecting at one fixed point. The fixed point describes a stable steady state. Two typical trajectories (dotted lines) are shown with arrow directions denoting increasing time.

The steady state is found to be stable over a wide range of parameter values. When  $\delta_1$  is  $\neq 0$  in equation (15), again over a wide range of parameter values there is only one physical steady state solution which is furthermore stable. Figure 7 shows the phase portrait obtained from equations (15) and (16) with the parameter values  $\alpha_1 = 2.5$ ,  $\alpha_3 = 50$ ,  $\mu_1 = 50$ ,  $\mu_2 = 10$ ,  $K_2 = 1000$ , and  $\delta_1 = 0.015$ . The nullclines, obtained by putting  $\frac{d(JA)}{dt} = 0$  and  $\frac{d(JZ)}{dt} = 0$ , intersect at a single point, the so-called fixed point of the dynamics. Two trajectories (shown by dotted lines) with two different initial conditions converge to the fixed point in the course of time. Each trajectory depicts the values of  $JA$  and  $JZ$  at different time points obtained by solving equations (15) and (16). Figure 8 shows the magnitude of  $JA$  versus time for the same parameter values. The transient pulse reaches a peak value due to an initial surge and the system finally settles down into a stable steady state with the value of  $JA$  much lower than the peak value.

### 3 Stochastic Dynamics

The single steady state characterized by a low value of  $JA$  is stable under small perturbations. Under sufficiently strong perturbations, a large-amplitude  $JA$  pulse is excited with eventual return to the stable steady state. The random nature of the biochemical events involved in gene expression gives rise to fluctuations in protein levels [25, 26] which act as perturbations. The simplest way to take the effect of fluctuations into account is to incorporate an additive noise term in either of the dynamical equations (15) and (16). The noise term further incorporates the effects of transient perturbations originating in wounding signals. The most prominent effect is obtained with the noise term added to equation (15). A possible reason for this is that  $JAZ$  represses the synthesis of both  $JA$  and  $JAZ$  so that fluctuations in the  $JAZ$  levels affect both the  $JA$  and  $JAZ$  levels. The stochastic dynamics are described by

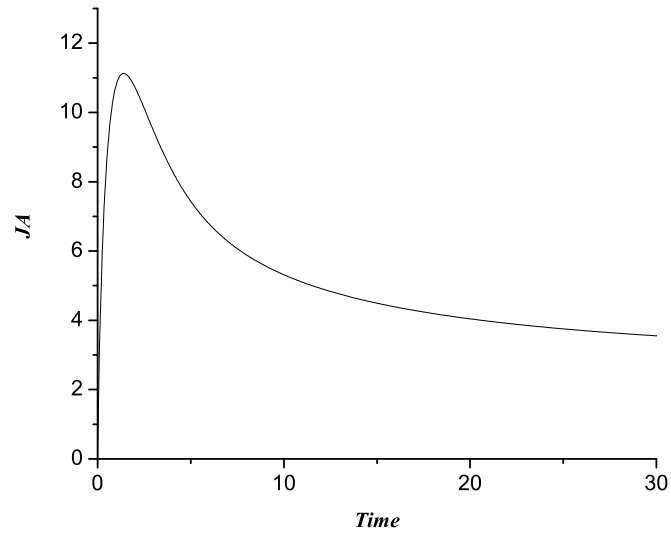


Figure 8: Transient pulse of  $JA$  versus time in the reduced model defined by equations (15) and (16).  $JA$  and time are dimensionless in the reduced model.

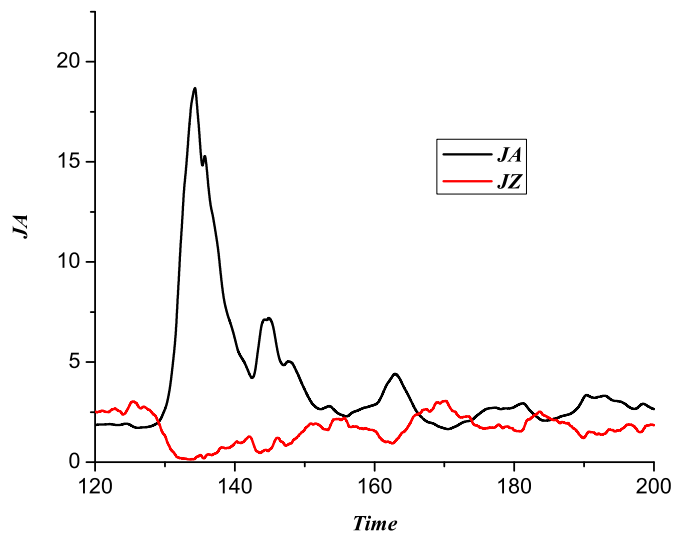


Figure 9: Variation of  $JA$  and  $JZ$  versus time in dimensionless units.

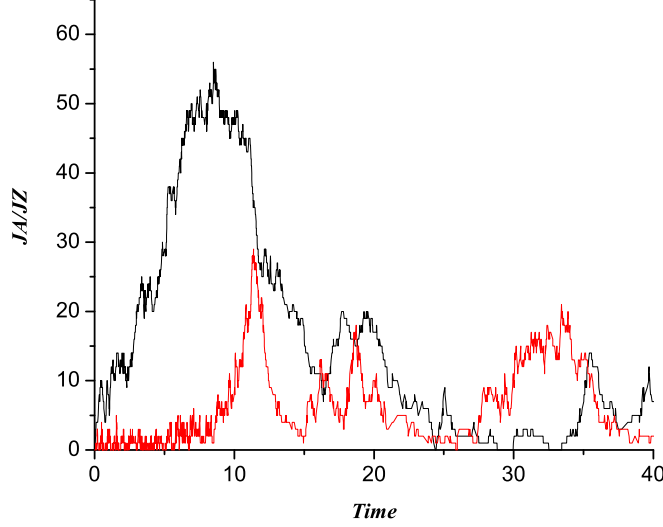


Figure 10: Number of JA (black curve) and JAZ (red curve) molecules versus time in hours. The values of the stochastic rate constants are mentioned in the text.

$$\frac{d(JZ)}{dt} = \frac{\alpha_1}{1 + \mu_1 JZ} - \frac{JA \cdot JZ}{JA + K_2 + JA \cdot JZ} - \delta_1 JZ + \xi(t) \quad (19)$$

$$\frac{d(JA)}{dt} = \frac{\alpha_2}{1 + \mu_2 JZ} - \delta_2 JA \quad (20)$$

The noise term  $\xi(t)$  approximates the actual fluctuations which occur in the system. We assume the noise to be of the Ornstein-Uhlenbeck(OU) type (coloured noise) [27, 28] as recent studies show that OU noise plays a significant role in gene expression dynamics [9, 29]. The noise variable has zero mean and an exponentially decaying correlation in time, i.e.,

$$\langle \xi(t) \rangle = 0 \quad (21)$$

$$\langle \xi(t) \xi(t') \rangle = D \lambda \exp(-\lambda |t - t'|) \quad (22)$$

where  $D$  is the noise strength and  $\lambda$  the inverse of the correlation time  $\tau$ . We use the numerical simulation algorithm developed for the OU process [30, 31] to obtain solutions of the stochastic differential equations (19) and (20). The major steps of the algorithm are as follows. Let  $x = JA$  and  $y = JZ$ . Knowing the values of  $x$  and  $y$  at time  $t$ , the values at time  $t + \Delta t$  ( $\Delta t$  is small) are

$$x(t + \Delta t) = x(t) + p \Delta t \quad (23)$$

$$y(t + \Delta t) = y(t) + q \Delta t \quad (24)$$

where

$$p = f(x, y) + \xi(t) \quad (25)$$

$$q = g(x, y) \quad (26)$$

The functions  $f(x, y)$  and  $g(x, y)$  are, from equation (19) and (20),

$$f(x, y) = \frac{\alpha_1}{1 + \mu_1 y} - \frac{x \cdot y}{x + K_2 + x \cdot y} - \delta_1 y \quad (27)$$

$$g(x, y) = \frac{\alpha_2}{1 + \mu_2 y} - x \quad (28)$$

The noise variable  $\xi(t + \Delta t)$  is

$$\xi(t + \Delta t) = \xi(t)\mu + \sigma_x n_1 \quad (29)$$

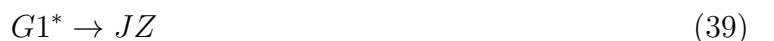
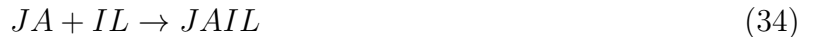
with

$$\mu = e^{-\lambda \Delta t} \quad (30)$$

$$\sigma_x^2 = D \lambda (1 - \mu^2) \quad (31)$$

and  $n_1$  is a normal random variable with mean zero and variance 1. Through iterative computation, using equations (23)-(31), the values of  $x$  and  $y$  at successive time steps  $\Delta t$  can be determined. Figure 9 shows the time traces of  $x(JA)$  and  $y(JZ)$  for the parameter values the same as in the cases of figures 7 and 8. The initial values of  $x$  and  $y$  are zero,  $\frac{1}{\lambda} = \tau = 0.5$  and  $D = 0.0625$ . The incremental time step  $\Delta t = 0.01$ . Figure 9 shows the anticorrelation between  $JA$  and  $JZ$  values, the  $JZ$  value dips when  $JA$  rises up to the peak pulse value. Fluctuations of moderate strength in  $JZ$  can give rise to transient  $JA$  pulses. With increased noise strength, transient pulses are more readily generated.

We further probe the stochastic dynamics of the full model with the help of computer simulation based on the Gillespie algorithm [32]. The reactions are 15 in number and are given by





The different symbols are explained in section 2.  $\phi$  denotes the proteins degradation product.  $G1$  ( $G2$ ) and  $G1^*$  ( $G2^*$ ) are the inactive and active states respectively of the gene synthesizing JAZ proteins (JA). The active state of the gene is attained on the binding of the transcription factor MYC2 to the regulatory region of the gene. For simplicity, only one JA biosynthesis gene is assumed. The stochastic rate constants, associated with the reactions, are  $C(i)$ ,  $i = 1, \dots, 15$  in appropriate units. Figure 10 shows the variation of the number of JA (black curve) and JAZ (red curve) molecules as a function of time. The values of the stochastic rate constants are  $C(1) = 0.2$ ,  $C(2) = 0.001$ ,  $C(3) = 0.1$ ,  $C(4) = 0.1$ ,  $C(5) = 0.1$ ,  $C(6) = 1.0$ ,  $C(7) = 1.0$ ,  $C(8) = 12.0$ ,  $C(9) = 10.0$ ,  $C(10) = 0.1$ ,  $C(11) = 0.4$ ,  $C(12) = 1.0$ ,  $C(13) = 1.0$ ,  $C(14) = 1.0$  and  $C(15) = 1.0$ . The stochastic time evolution of  $JA$  shows a transient pulse of large amplitude followed by a series of small amplitude transient pulses. As in the case of the reduced model, the JA and JZ values are anticorrelated.

## 4 Conclusion and Outlook

The JA signaling pathway is activated in defending plants against attacks by pathogens and wounding by animals. Recent experiments [4, 5, 6] provide important new knowledge on the molecular connectivity of the pathway. The observations suggest a model in which two feedback loops, one positive and the other negative, control the dynamics of JA response in the form of a transient pulse. In this paper, we propose a minimal mathematical model which captures the essential features of the JA signaling pathway. To our knowledge, no other mathematical model of the dynamics of the coupled feedback loops in the JA signaling pathway has been proposed so far. The model demonstrates the formation of the transient JA pulse for different parameter values. The pulse is an outcome of two opposing influences mediated via the positive and negative feedback loops. We compute the dependence of the pulse amplitude, duration and peak time on the key parameters of the theoretical model. The full mathematical model, described in terms of equations (4)-(8), can be reduced to a two-variable model (equations (15) and (16)) for which the physical steady state solution is obtained analytically. There is only one such solution, corresponding to low JA levels, which is stable in an extended region of the parameter space. A similar conclusion holds

true for the full dynamical model. We explore the dynamics of both the full and reduced models using deterministic as well as stochastic formalisms. The TF MYC2 activates the expression of both the JA biosynthesis and JAZ genes. In normal circumstances, the expression activity is low as JAZ proteins repress MYC2 by forming bound complexes with the TF proteins. For the JA pulse to be initiated, free MYC2 is required. Once the JA synthesis is initiated, the positive feedback loop ramps up further JA production. The negative feedback loop acts against the enhancement so that the JA level attains a steady lower value after a certain time interval. JA-mediated destruction of JAZ repressors frees MYC2 which in turn activates JAZ gene expression. The production of JAZ proteins completes the negative feedback loop through the repression of MYC2 activity (figure 1). In the deterministic formalism, the transient JA pulse is obtained when a certain amount of free MYC2 is available at time  $t = 0$ . The availability of free MYC2 is JA-dependent. We do not model the explicit steps of JA biosynthesis and the synthesis of MYC2. We study the dynamics of the JA signaling pathway with free MYC2 as input. The central role of MYC2 in the model is dictated by available experimental evidence but there could be other TFs playing similar roles (see figure 5(b) of [33]). The prominent role of MYC2 could be tested experimentally by adding free MYC2 to plant leaves and checking whether transient JA pulses are obtained even in the absence of wounding. In the stochastic case, fluctuations in the numbers of JA and JAZ proteins can activate pulse formation. This is clearly understood in the framework of the reduced model. As figure 9 distinctly shows, the fluctuations in JA and JAZ numbers are anticorrelated. A temporary dip in the JAZ levels results in the increased availability of free MYC2 and the subsequent generation of a JA pulse. Single cell experiments on a variety of organisms have established the stochastic nature of gene expression [25, 26] and it is now common knowledge that protein fluctuations have a considerable effect on cellular processes.

The operating principle behind transient gene expression activity in the JA signaling pathway is based on a combination of positive and negative feedback loops and the availability of free MYC2 to transactivate the expression of the JA biosynthesis and JAZ genes. Due to the transient nature of the JA pulse, individual cells attain a state in which elevated levels of JA induce the expression of target genes involved in defense response and after a time interval return to the quiescent state. In *B. subtilis*, a core module consisting of positive and negative feedback loops can explain transient gene expression activity resulting in entry into the competent state and subsequent exit from it [9]. The dynamics, however, have features different from those in the case of the JA signaling pathway. The ComK proteins autoactivate their own production in a cooperative fashion, i.e., bound complexes of ComK activate the initiation of transcription of the *comK* gene. The analysis of the dynamics reveals three physical fixed points: a stable fixed point at low ComK concentration ( the vegetative state), one unstable saddle fixed point at intermediate ComK and an unstable spiral at high ComK ( the competent state) [9]. The system exhibits excitable dynamics in which relatively small perturbations of the low ComK vegetative state can initiate long excursions in phase space around the unstable spiral node, resulting in transient activation of the competent state. Since the intermediate and high ComK fixed points are unstable, the system ultimately returns to the stable vegetative state. In contrast, the dynamics of JA pulse formation involve only one fixed point. A similar situation prevails in the case of the HIV regulatory circuit. A minimal model of the circuit dynamics predicts a single fixed point which is stable provided a specific condition is satisfied [12]. In this case, the long-lived pulse of Tat proteins results from transient positive feedback amplification and deactivation via stronger back reactions like deacetylation of the Tat protein and unbinding of the regulatory molecules. The back reactions opposing the action of the positive feedback loop have an effective influence similar to that of a negative feedback loop. The operating principle in the HIV circuit is that of feedback resistor, analogous to the presence



of a dissipative resistor in an electrical feedback circuit. The dissipative resistor stabilizes the low expression state of a positive feedback loop.

In *B. subtilis*, fluctuations in ComK levels trigger competence development in a fraction of cells, demonstrated explicitly in the stochastic dynamics of the minimal model describing competence development [9]. There is now experimental validation of the proposal that noise in gene expression determines cell fate in *B. subtilis* [10]. In the Tat circuit, stochastic molecular fluctuations intrinsic to gene expression can activate transient Tat pulses. The feedback resistor model, however, shows that the off state is quite stable and more robust to noise than cooperative positive feedback loops. The inherent noise buffering is due to the presence of “dissipative resistors” in the transactivation circuit [12]. The phenotypic diversity observed in isogenic HIV-1 virus populations is ascribed to desynchronized Tat pulses in individual cells due to stochastic gene expression. In the case of the JA signaling pathway, noise-induced activation of the JA pulse is possible (figures 9 and 10) but the off state is found to be quite stable to fluctuations in the stochastic simulation of the reduced (figure 9) and full (figure 10) models. The negative feedback, analogous to the feedback resistor, enhances the off-state stability in this case.

An interesting aspect of JA-response not addressed in the present study relates to memory formation of past wounding events or attacks priming plants for a more effective JA-mediated defense response to subsequent attacks [34, 35]. Evidence of memory formation could lie in the modification of (1) the peak time of JA accumulation, (2) amplitude of JA pulse or (3) baseline of accumulated JA due to discrete JA bursts elicited by repeated attacks [34]. The negative feedback loop **b** in the JA-signaling network constitutes a well-known motif in gene regulatory networks. A negative feedback loop by itself may give rise to oscillatory dynamics or alternatively pulsed protein production [36, 37]. The *p53 – MDM2* loop provides a well-known example of negative feedback [36]. The loop is functionally active in response to DNA damage. Single cell experiments show that on DNA damage by  $\gamma$ -irradiation a series of undamped p53 pulses of fixed amplitude and duration is generated. The amount of  $\gamma$ -irradiation determines the number of pulses but has no effect on the amplitude and duration of the pulses. The functional response of the MYC2-JAZ negative feedback loop in the JA signaling pathway to wounding signals of varying magnitude is worth exploring at the single cell level to gain insight on key dynamical features. It is generally difficult to link circuit dynamics with circuit structure. The identification of feedback loops in the JA signaling pathway allows for the construction of a minimal mathematical model which correctly reproduces the formation of JA pulses on activation. The deterministic and stochastic origins of pulse formation are obtained through computational analysis. The dependence of key pulse parameters on the kinetic rate constants is demonstrated quantitatively. Further experiments are needed to validate the theoretical predictions as well as to elucidate the operating principle of the JA signaling pathway at a microscopic level. Comparative studies of operating principles controlling transient gene expression activity in diverse organisms are expected to provide insight on the common mechanisms organisms living in a complex environment adopt for responding to stress signals.

## References

- [1] Browse J 2009 Jasmonate Passes Muster: A Receptor and Targets for the Defense Hormone *Annu. Rev. Plant Biol.* 60 183-205
- [2] Devoto A and Turner J G 2003 Regulation of Jasmonate-mediated Plant Responses in *Arabidopsis* *Ann. Bot. (Lond.)* 92 329-37

- [3] Lorenzo O and Solano R Molecular players regulating the jasmonate signalling network *Curr. Opin. Plant Biol.* 8 532-40
- [4] Farmer E E, Almeras E and Krishnamurthy V 2003 Jasmonates and related oxylipins in plant responses to pathogenesis and herbivory *Curr. Opin. Plant Biol.* 6 372-378
- [5] Chini A et al. 2007 The JAZ family of repressors is the missing link in jasmonate signalling *Nature* 448 666-71
- [6] Thines B et al. The JAZ repressor proteins are targets of the *SCF<sup>COI1</sup>* complex during jasmonate signalling *Nature* 448 661-65
- [7] Farmer E E 2007 Jasmonate perception machines *Nature* 448 659-660
- [8] Smits W K et al. 2005 Stripping Bacillus: ComK auto-stimulation is responsible for the bistable response in competence development *Mol. Microbiol.* 56 604-14
- [9] Süel G M, Garcia - Ojalvo J, Liberman L M and Elowitz M B 2006 An excitable gene regulatory circuit induces transient cellular differentiation *Nature* 440 545-50
- [10] Maamar H, Raj A and Dubnau D 2007 Noise in gene expression determines cell fate in *Bacillus subtilis* *Science* 2007 317 526-29
- [11] Weinberger L S, Burnett J C, Toettcher J E, Arkin A P and Schaffer D V 2005 Stochastic gene expression in a lentiviral positive-feedback loop: HIV-1 Tat fluctuations drive phenotypic diversity *Cell* 122 169–182
- [12] Weinberger L S and Shenk T 2007 An HIV feedback resistor: auto-regulatory circuit deactivator and noise buffer *PLOS Biol.* 5 0067-81
- [13] Weinberger L S, Dar R D and Simpson M L 2008 Transient-mediated fate determination in a transcriptional circuit of HIV *Nature Genetics* 40 466 - 470
- [14] Shin D, Lee E-Jin, Huang H and Groisman E A 2006 A Positive Feedback Loop Promotes Transcription Surge That Jump-Starts Salmonella Virulence Circuit 314 1607-09
- [15] Koo A J K and Howe G A 2009 The wound hormone jasmonate *Phytochemistry* 70 1571-80
- [16] Staswick P E 2008 JAZing up jasmonate signaling *Trends Plant Sci.* 13:66-71.
- [17] Chini A, Boter M and Solano R Plant oxylipins: COI1/JAZs/MYC2 as the core jasmonic acid-signalling module *FEBS Journal* 276 4682 - 4692
- [18] Chung H S, Niu Y Browse J and Howe G A 2009 Top hits in contemporary JAZ: An update on jasmonate signaling *Phytochemistry* 70 1547-59
- [19] Yan J et al. 2009 The Arabidopsis CORONATINE INSENSITIVE1 Protein Is a Jasmonate Receptor *The Plant Cell* 21 2220-2236
- [20] Wasternack C 2007 Jasmonates: An Update on Biosynthesis, Signal Transduction and Action in Plant Stress Response, Growth and Development *Annals of Botany* 2 1-17

- [21] Pauwels L and Goossens A 2008 Fine-tuning of early events in the jasmonate response *Plant signalling and Behaviour* 3 846 - 847
- [22] Lorenzo O, Chico J M, Sánchez-Serrano J J and Solano R 2004 JASMONATE-INSENSITIVE1 encodes a MYC transcription factor essential to discriminate between different jasmonate-regulated defense responses in Arabidopsis *Plant Cell* 16 1938-50
- [23] Chung H S et al. 2008 Regulation and Function of Arabidopsis JASMONATE ZIM-Domain Genes in Response to Wounding and Herbivory *Plant Physiol* 146 952-64
- [24] Glauser G, Grata E, Dubugnon L, Rudaz S, Farmer E E and Wolfender J L 2008 Spatial and temporal dynamics of jasmonate synthesis and accumulation in Arabidopsis in response to wounding *J. Biol. Chem.* 283 16400-407
- [25] Kaern M, Elston T C, Blake W J and Collins J J 2005 Stochasticity in gene expression: from theories to phenotypes *Nat Rev Genet.* 6 451-64
- [26] Raj A and van Oudenaarden A 2008 Nature, Nurture, or Chance: Stochastic Gene Expression and Its Consequences *October* 6 216-226
- [27] van Kampen N G 1992 *Stochastic Processes in Physics and Chemistry* (North-Holland, Amsterdam)
- [28] Chandrasekhar S 1943 Stochastic Problems in Physics and Astronomy *Rev. Mod. Phys.* 15 1-89
- [29] Rosenfeld N, Young J W, Alon U, Swain P S and Elowitz M B 2005 Gene regulation at the single-cell level *Science* 307 1962-5
- [30] Fox R F, Gatland I R, Roy R and G. Vemuri 1998 Fast, accurate algorithm for numerical simulation of exponentially correlated colored noise *Phys. Rev. A* 38 5938-40
- [31] Gillespie D T 1996 Exact numerical simulation of the Ornstein-Uhlenbeck process and its integral *Phys. Rev. E* 54 2084 - 2091
- [32] Gillespie D T 1977 Exact stochastic simulation of coupled chemical reactions *J. Phys. Chem* 81 2340-61
- [33] Pieterse C M J, Leon-Reyes A, Sjoerd Van der Ent & Saskia C M Van Wees 2009 Networking by small-molecule hormones in plant immunity *Nature Chem. Biol.* 5 308-16
- [34] Gális I, Gaquerel E, Pandey S P and Baldwin I T 2009 Molecular mechanisms underlying plant memory in JA-mediated defence responses *Plant Cell Environ.* 32(6) 617-27
- [35] Stork W, Diezel C, Halitschke R, Gális I nad Baldwin I T 2009 An Ecological Analysis of the Herbivory-Elicited JA Burst and Its Metabolism: Plant Memory Processes and Predictions of the Moving Target Model *PLOS ONE* e 4697
- [36] Novák B and Tyson J J 2008 Design principles of biochemical oscillators *Nature Rev Mol. Cell Biol.* 2008 9 981-91
- [37] Batchelor E , Loewer A and Lahav G 2009 The ups and downs of p53: understanding protein dynamics in single cells *Nature Rev. Cancer* 9 371-377

## Figure Captions

1. Core components of the JA signaling pathway [7]. Transcription factor (TF), MYC2, activates the synthesis of both JA and JAZ. The arrow sign denotes activation and the hammerhead sign repression. The function of the components is described in the text.
2. Transient pulse of JA versus time in hours.  $JA$  has the unit of concentration.
3. Variation of JA versus time in hours for values of  $\beta_2 = 10, 20, 30$  and  $40$ . The peak height of the pulse increases for increasing values of  $\beta_2$ .  $JA$  has the unit of concentration.
4. Variation of  $JA$  versus time for different values of  $\beta_1 = 5, 10, 20, 30$  and  $40$ .
5. Amplitude of JA pulse versus (a)  $\beta_1$  and (b)  $\beta_2$ ; Peak time  $t_m$  in hours of the JA pulse versus (c)  $\beta_1$  and (d)  $\beta_2$ ; Duration  $t_D$  in hours of JA pulse versus (e)  $\beta_1$  and  $\beta_2$ .
6. Variation of  $JA$  versus time in hours for different values  $\gamma_2 = 0.1, 0.2, 0.3$  and  $0.4$  of the degradation rate constant. The amplitude of the JA pulse decreases for increasing value of  $\gamma_2$ .  $JA$  has the unit of concentration.
7. Phase portrait defined by equations (15) and (16). The solid lines represent the nullclines( $\frac{d(JA)}{dt} = 0$ (red),  $\frac{d(JZ)}{dt} = 0$ (black)) intersecting at one fixed point. The fixed point describes a stable steady state. Two typical trajectories (dotted lines) are shown with arrow directions denoting increasing time.
8. Transient pulse of JA versus time in the reduced model defined by equations (15) and (16).  $JA$  and time are dimensionless in the reduced model.
9. Variation of  $JA$  and  $JZ$  versus time in dimensionless units.
10. Number of JA (black curve) and JAZ (red curve) molecules versus time in hours. The values of the stochastic rate constants are mentioned in the text.